

Introduction to Density Functional Theory with Applications to Graphene

Branislav K. Nikolić

Department of Physics and Astronomy, University of Delaware,
Newark, DE 19716, U.S.A.

<http://wiki.physics.udel.edu/phys824>



Band Structure of Graphene: Tight-Binding vs. Ab Initio

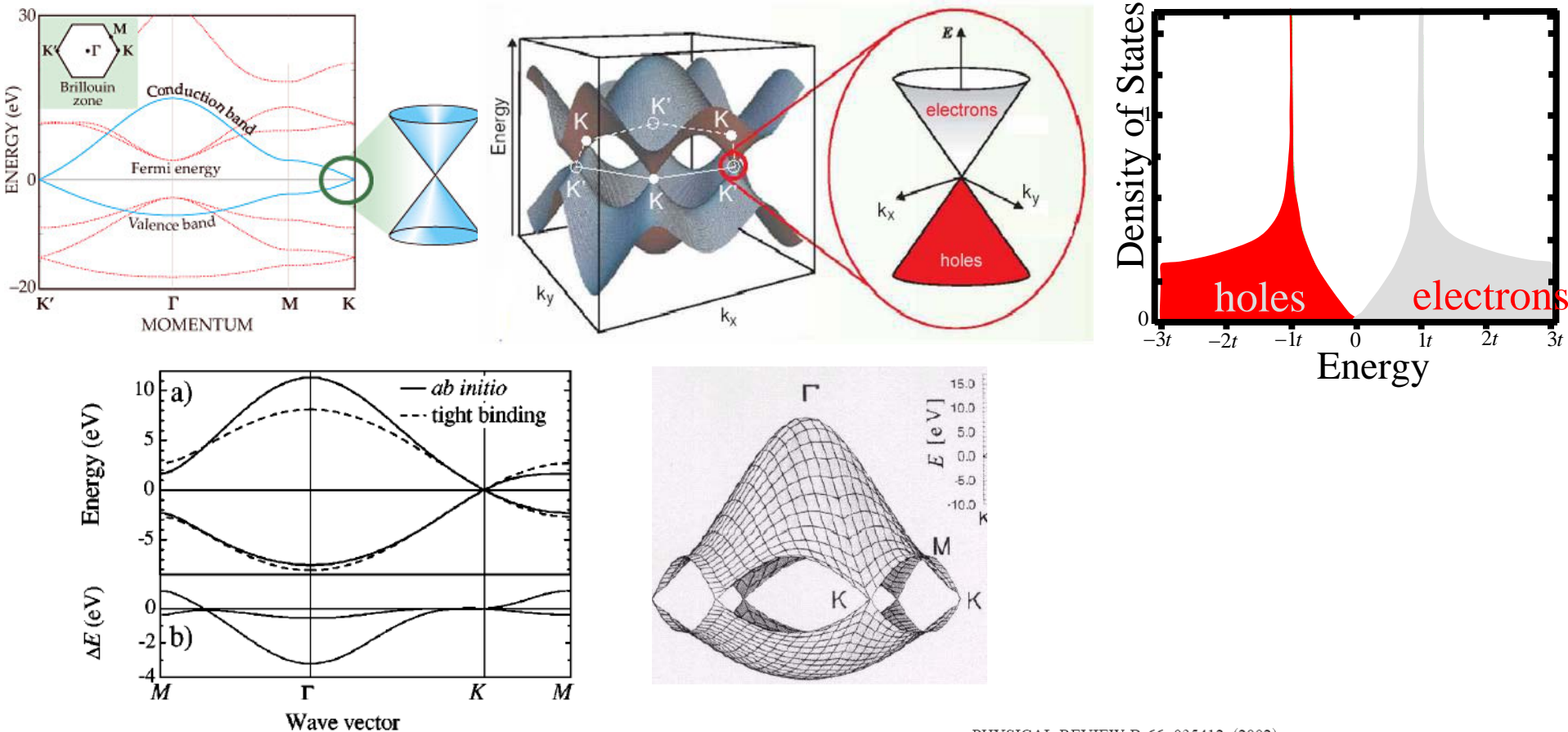


FIG. 2. *Ab initio* and nearest-neighbor tight-binding dispersions of graphene. (a) The converged *ab initio* calculation of the graphene π and π^* electronic bands is shown by the full lines. The dashed lines represent the tight-binding dispersion of Eq. (6) with $s_0=0$ and $\gamma_0=-2.7$ eV. (b) Difference ΔE between the *ab initio* and tight-binding band structures.

PHYSICAL REVIEW B 66, 035412 (2002)

Tight-binding description of graphene

S. Reich, J. Maultzsch, and C. Thomsen

Institut für Festkörperphysik, Technische Universität Berlin, Hardenbergstrasse 36, 10623 Berlin, Germany

P. Ordejón

Institut de Ciència de Materials de Barcelona (CSIC), Campus de la U.A.B. E-08193 Bellaterra, Barcelona, Spain

DFT Provides Parameters for Empirical Tight-Binding Hamiltonians

PHYSICAL REVIEW B 66, 035412 (2002)

Tight-binding description of graphene

S. Reich, J. Maultzsch, and C. Thomsen

Institut für Festkörperphysik, Technische Universität Berlin, Hardenbergstrasse 36, 10623 Berlin, Germany

P. Ordejón

Institut de Ciència de Materials de Barcelona (CSIC), Campus de la U.A.B. E-08193 Bellaterra, Barcelona, Spain

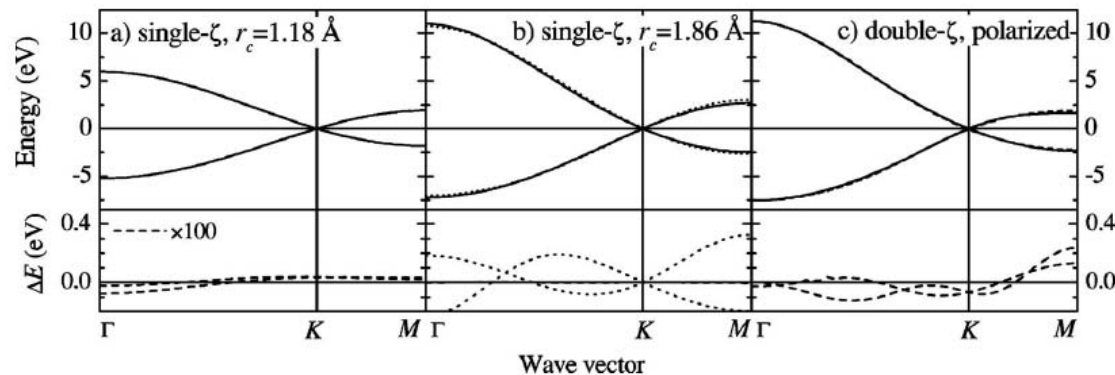
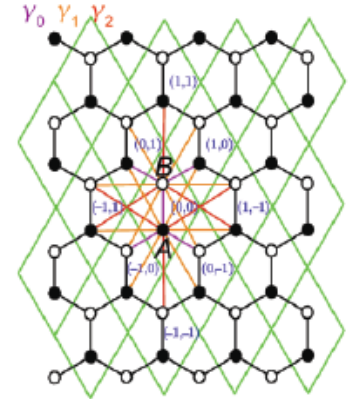
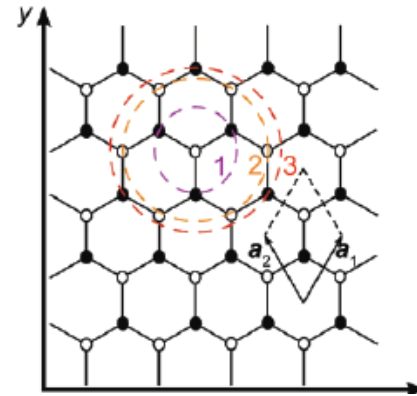


FIG. 3. (a) Top: first-principles band structure with a single- ζ basis set and $r_c = 1.18$ Å. The nearest-neighbor tight-binding band structure [Eq. (6)] with $\gamma_0 = -1.86$ eV and $s_0 = 0.02$ coincides with the first-principles result. Bottom: difference ΔE between the first-principles and nearest-neighbor tight-binding band structures. (b) Top, full lines: first-principles result with a single- ζ basis set and $r_c = 1.86$ Å; dotted lines: nearest-neighbor tight-binding band structure [Eq. (6)] with $\gamma_0 = -2.84$ eV and $s_0 = 0.070$; the third-nearest neighbor tight-binding band structure coincides with the first-principles result shown by the full lines ($\epsilon_{2p} = -0.36$ eV, $\gamma_0 = -2.78$ eV, $\gamma_1 = -0.12$ eV, $\gamma_2 = -0.068$ eV, $s_0 = 0.106$, $s_1 = 0.001$, and $s_2 = 0.003$). Bottom, dotted line: difference between the first-principles and the nearest-neighbor tight-binding band structure shown in the top panel. For the third-nearest neighbor tight-binding approximation the differences are not seen on the chosen energy scale. (c) Top: converged *ab initio* (full lines) and third-neighbor tight-binding (dashed) band structures; see Table I for the tight-binding parameters ($M\Gamma KM$). Bottom: difference between the two band structures above.

DFT Band Structure vs. Simple Models of Ferromagnetism

Journal of Magnetism and Magnetic Materials 320 (2008) 1190–1216

Current Perspectives

Spin transfer torques

D.C. Ralph^{a,*}, M.D. Stiles^b

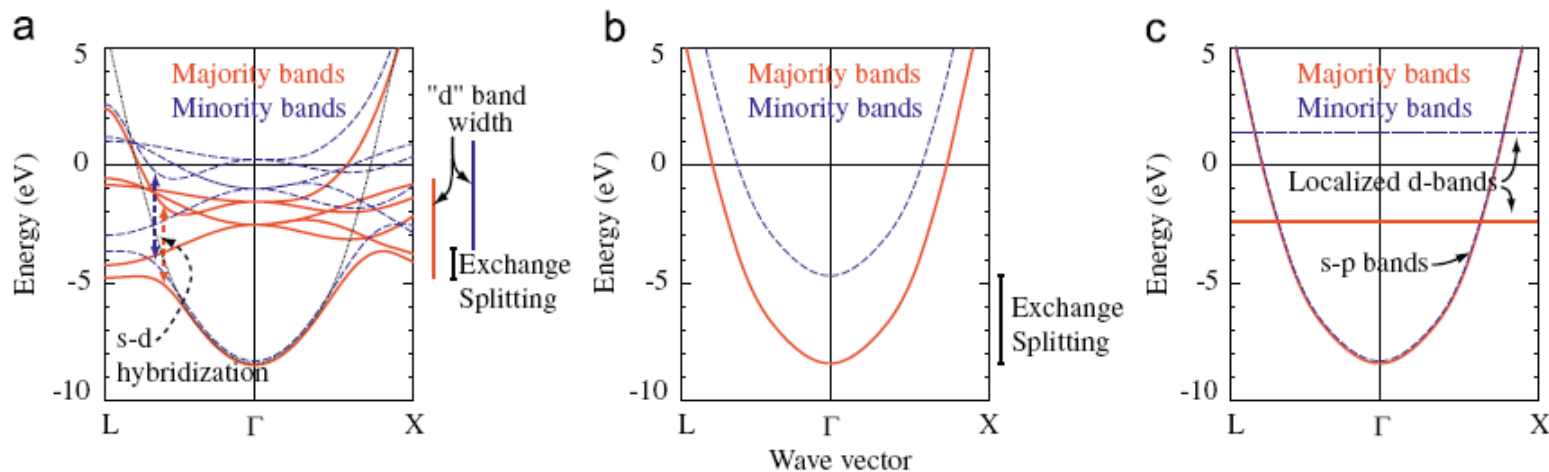
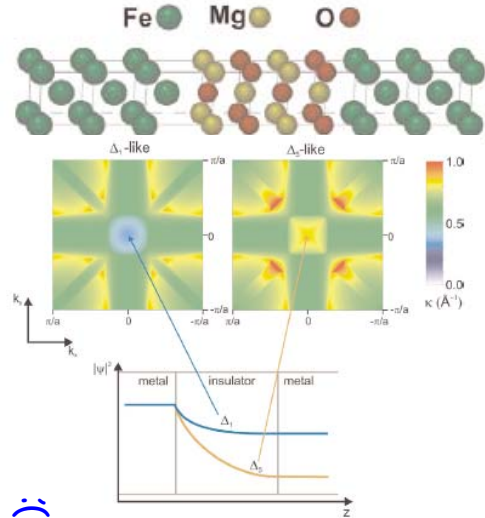
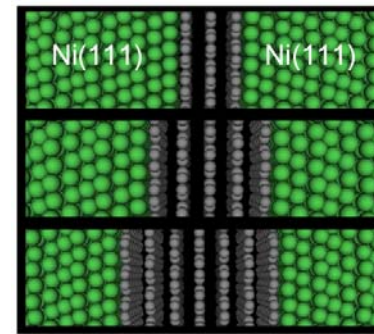


Fig. 4. Model band structures for ferromagnets. The solid red (dashed blue) curves give the majority (minority) bands along two high symmetry directions through the Brillouin zone center, Γ . Panel (a) gives bands calculated in the LSDA for face-centered cubic (fcc) Co. The dotted black curve shows what the energy of the s-p band would be if it were not hybridized with the d bands. The bars to the right of (a) show the width of the d bands and the shift between the majority and minority bands. The dashed arrows in (a) indicated the widths of avoided level-crossings due to the hybridization between the s-p and d bands of the same symmetry along the chosen direction. Panel (b) gives a schematic version of a Stoner model for a ferromagnet. The exchange splitting is larger than in (a) in order to produce a reasonable size moment. The majority and minority Fermi surfaces are more similar to each other than they are for the LSDA model. Panel (c) gives a schematic s-d model band structure. The current-carrying s-p bands have a very small splitting due to the weak exchange interaction with the localized d-states. The majority and minority Fermi surfaces are almost identical.

DFT in the Quest for Perfect MTJs: Fe|MgO|Fe and Ni|Graphene|Ni

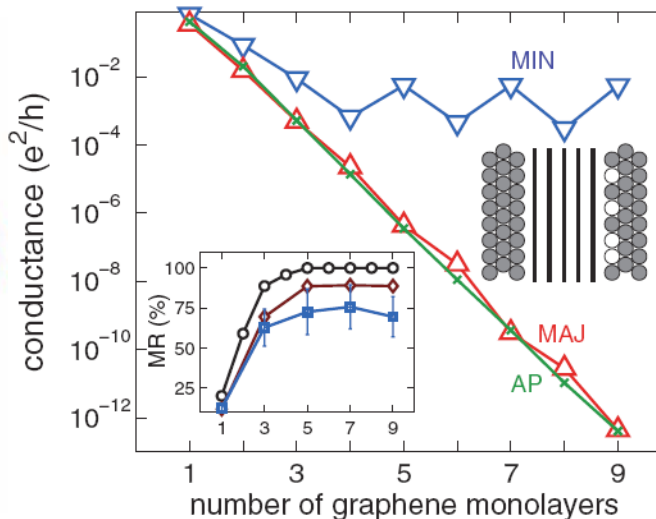
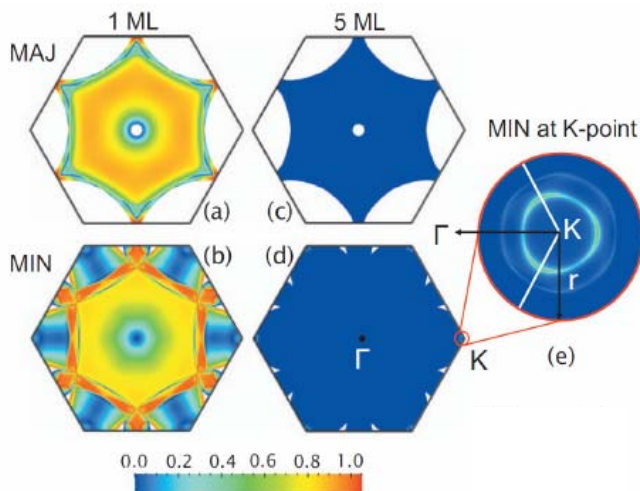
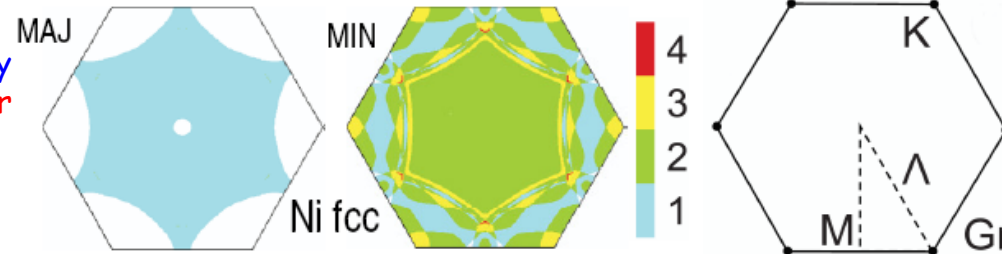


DFT Preliminary Analysis:
 In-plane lattice constant of graphene matches the surface lattice constants of Ni(111) almost perfectly → The only electronic states at or close to the Fermi energy are near the high symmetry K point in the Brillouine zone where Ni has states with minority spin character only
 → Perfect spin filtering for this interface (in the absence of defects, disorder, and interface reconstruction).



Graphite	$a_{\text{hex}} = 2.46 \text{ \AA}$
Co	$a_{\text{hex}} = 2.42 \text{ \AA}$
Ni	$a_{\text{hex}} = 2.49 \text{ \AA}$
Cu	$a_{\text{hex}} = 2.57 \text{ \AA}$

Ni-Gr mismatch only 1.3%



$$\text{TMR}_{\text{pessimistic}} = \frac{G^P - G^{AP}}{G^P + G^{AP}}$$

$$\text{TMR}_{\text{optimistic}} = \frac{G^P - G^{AP}}{G^{AP}}$$

TMR (tunnel magneto-resistance)

1 layer = 38%	R.A ($\Omega\mu\text{m}^2$) = 0.004
5 layer = 105%	R.A ($\Omega\mu\text{m}^2$) = 0.23
7 layer = 107%	R.A ($\Omega\mu\text{m}^2$) = 0.5

Kelly Ggoup, PRL 99, 176602 (2007);
 PRB 78, 195419 (2008).

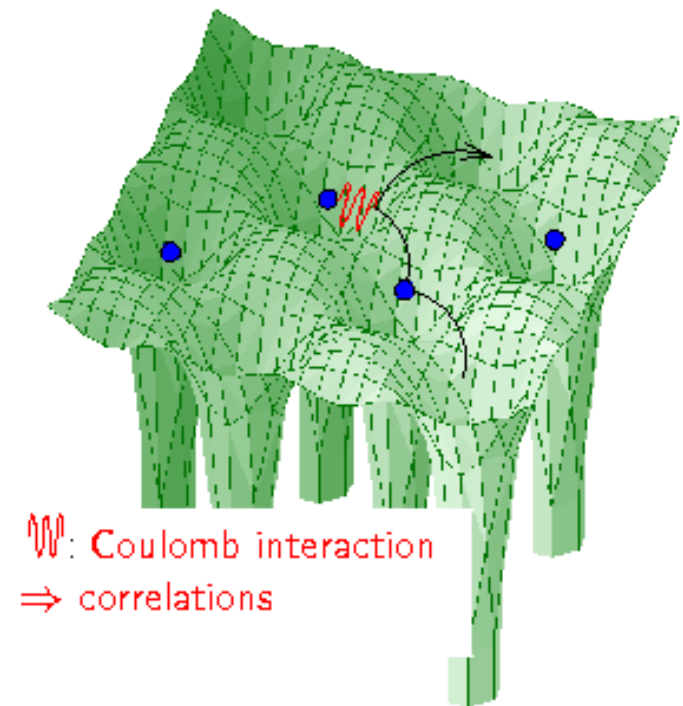
Quantum-Mechanical Many-Body Problem for Electrons in Solids

□ Hamiltonian of electrons in solid after Born-Oppenheimer approximation:

$$\hat{H} = \sum_i \left[-\frac{\hbar^2 \Delta_i}{2m_e} + \sum_l \frac{-e^2}{4\pi\epsilon_0} \frac{Z_l}{|\mathbf{r}_i - \mathbf{R}_l|} \right] + \frac{1}{2} \sum_{i \neq j} \frac{e^2}{4\pi\epsilon_0} \frac{1}{|\mathbf{r}_i - \mathbf{r}_j|}.$$

Solid State Hamiltonian:

To calculate material properties, one has to take into account three terms: The kinetic energy favoring the electrons to move through the crystal (blue), the lattice potential of the ions (green), and the Coulomb interaction between the electrons (red). Due to the latter, the first electron is repelled by the second, and it is energetically favorable to hop somewhere else, as depicted. **Hence, the movement of every electron is correlated with that of every other, which prevents even a numerical solution.**



Density Functional Theory Approach to Quantum Many-Body Problem

□ Conventional Quantum Mechanical approach to many-body systems:

$$v(\mathbf{r}) \xrightarrow{SE} \Psi(\mathbf{r}_1, \mathbf{r}_2, \dots, \mathbf{r}_N) \xrightarrow{\langle \Psi | \dots | \Psi \rangle} \text{observables}$$

$$E_{v,0} = E_v[\Psi_0] = \langle \Psi_0 | \hat{H} | \Psi_0 \rangle \leq \langle \Psi' | \hat{H} | \Psi' \rangle = E_v[\Psi']$$

$$n(\mathbf{r}) = N \int d^3r_2 \int d^3r_3 \dots \int d^3r_N \Psi^*(\mathbf{r}, \mathbf{r}_2, \dots, \mathbf{r}_N) \Psi(\mathbf{r}, \mathbf{r}_2, \dots, \mathbf{r}_N)$$

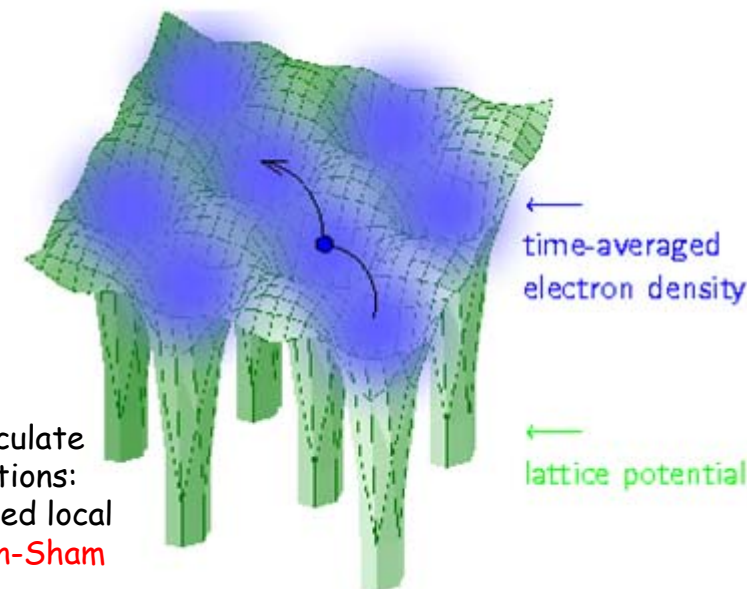
□ DFT conceptual structure:

$$n(\mathbf{r}) \implies \Psi(\mathbf{r}_1, \dots, \mathbf{r}_N) \implies v(\mathbf{r})$$

Knowledge of electron density implies knowledge of the wave function and the potential, and hence of all other observables. Although this sequence describes the conceptual structure of DFT, it does not really represent what is done in actual applications of it, which typically proceed along rather different lines, and do not make explicit use of many-body wave functions

□ DFT in computational practice:

Local Density Approximation (LDA) is an approximation which allows to calculate material properties but which dramatically simplifies the electronic correlations: Every electron moves independently, i.e., uncorrelated, within a time-averaged local density of the other electrons, as described by a set of **single-particle Kohn-Sham equations** whose solutions ("orbitals") are used to build the density.



Computational Complexity: Many-Body Wave Function vs. Electron Density vs. KS Orbitals

A Bird's-Eye View of Density-Functional Theory

Klaus Capelle

Departamento de Física e Informática

Instituto de Física de São Carlos

Universidade de São Paulo

Caixa Postal 369, São Carlos, 13560-970 SP, Brazil

⁶A simple estimate of the computational complexity of this task is to imagine a real-space representation of Ψ on a mesh, in which each coordinate is discretized by using 20 mesh points (which is not very much). For N electrons, Ψ becomes a function of $3N$ coordinates (ignoring spin, and taking Ψ to be real), and 20^{3N} values are required to describe Ψ on the mesh. The density $n(\mathbf{r})$ is a function of three coordinates, and requires 20^3 values on the same mesh. CI and the Kohn-Sham formulation of DFT additionally employ sets of single-particle orbitals. N such orbitals, used to build the density, require $20^3 N$ values on the same mesh. (A CI calculation employs also unoccupied orbitals, and requires more values.) For $N = 10$ electrons, the many-body wave function thus requires $20^{30}/20^3 \approx 10^{35}$ times more storage space than the density, and $20^{30}/(10 \times 20^3) \approx 10^{34}$ times more than sets of single-particle orbitals. Clever use of symmetries can reduce these ratios, but the full many-body wave function remains inaccessible for real systems with more than a few electrons.

DFT is Based on the Exact Hohenberg-Kohn Theorem

1. The nondegenerate ground-state (GS) wave function is a unique functional of the GS density:

$$\Psi_0(\mathbf{r}_1, \mathbf{r}_2 \dots, \mathbf{r}_N) = \Psi[n_0(\mathbf{r})]$$

2. The GS energy, as the most important observable, has variational property:

$$E_{v,0} = E_v[n_0] = \langle \Psi[n_0] | \hat{H} | \Psi[n_0] \rangle$$

$$E_v[n_0] \leq E_v[n']$$

3. Kinetic energy and electron-electron interaction energy are universal (system independent) functionals of electron density:

$$E_v[n] = T[n] + U[n] + V[n] = F[n] + V[n]$$

while non-universal potential energy in external field is obtained from:

$$V[n] = \int d^3r n(\mathbf{r}) v(\mathbf{r})$$

4. If external potential $v(\mathbf{r})$ is not held fixed, the functional $V[n]$ becomes universal: the GS density determines not only the GS wave function Ψ_0 , but, up to an additive constant, also the potential $V[n_0]$. **CONSEQUENCE:**

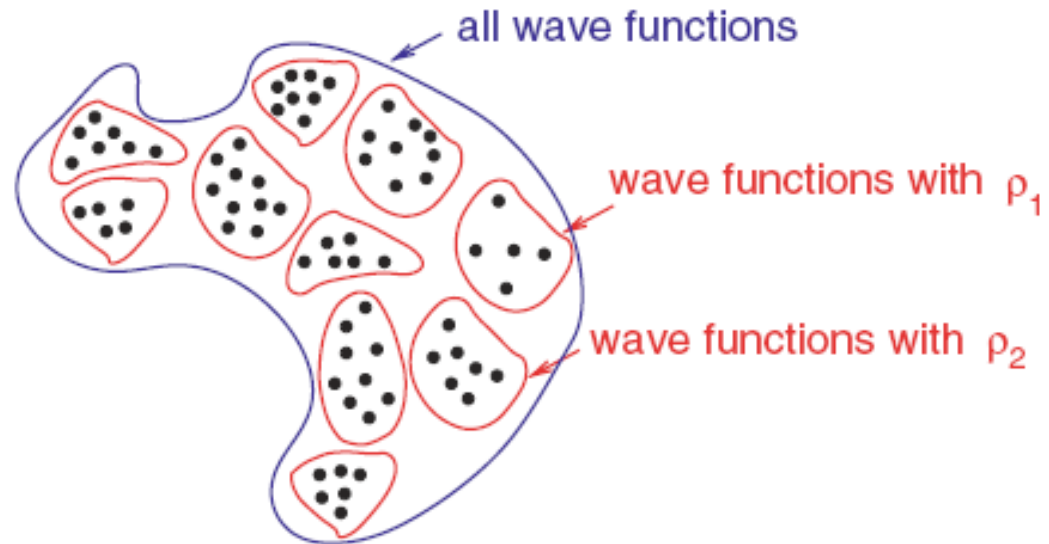
$$E_0 = E[n_0] = \langle \Psi[n_0] | \hat{T} + \hat{U} + \hat{V}[n_0] | \Psi[n_0] \rangle$$

$$\Psi_k(\mathbf{r}_1, \mathbf{r}_2 \dots, \mathbf{r}_N) = \Psi_k[n_0]$$

Two Step Formal Construction of the Energy Density Functional

$$E[n] = \min \left\{ \langle \Psi | \hat{H} | \Psi \rangle \mid \langle \Psi | \sum_{i=1}^N \delta(\mathbf{r} - \mathbf{r}_i) | \Psi \rangle = n(\mathbf{r}) \right\}$$

$$E_0 = \min_n E[n]$$



□ While this construction proves the Hohenberg-Kohn theorem, we did not actually gain anything: to obtain the functional $E[n]$ we have to calculate the expectation value $\langle \Psi | \hat{H} | \Psi \rangle$ for complicated many-body wave functions $\Psi(\mathbf{r}_1\sigma_1, \dots, \mathbf{r}_N\sigma_N)$.

Functionals and Functional Derivatives

□ Function vs. Functional:

$x \mapsto f(x)$ function maps number to a number

$n(\mathbf{r}) \mapsto F[n]$ functional maps whole function to a number; example:

$$N = \int d^3\mathbf{r} n(\mathbf{r}) = N[n]$$

$F[n(\mathbf{r})]$ is the same as $F[n(\mathbf{r}')]$

□ Standard Derivative vs. Functional Derivative:

$$f(x + dx) = f(x) + \frac{df}{dx}dx + O(dx^2)$$

$$F[f(x) + \delta f(x)] = F[f(x)] + \int dx \frac{\delta F[f]}{\delta f(x)} \delta f(x) + O(\delta f^2)$$

the integral arises
because the variation in
the functional F is
determined by variations
in the function at all
points in space

□ Useful formula:

$$F[n] = \int f(n, n', n'', n''', \dots; x) dx \Rightarrow \frac{\delta F[n]}{\delta n(x)} = \frac{\partial f}{\partial n} - \frac{d}{dx} \frac{\partial f}{\partial n'} + \frac{d^2}{dx^2} \frac{\partial f}{\partial n''} - \frac{d^3}{dx^3} \frac{\partial f}{\partial n'''} + \dots$$

Example from classical
mechanics:

$$\mathcal{A}[q] = \int \mathcal{L}(q, \dot{q}; t) dt \Rightarrow 0 = \frac{\delta \mathcal{A}[q]}{\delta q(t)} = \frac{\partial \mathcal{L}}{\partial q} - \frac{d}{dt} \frac{\partial \mathcal{L}}{\partial \dot{q}}$$

Practical DFT: Kohn-Sham Equations

□ Only the ionic (external for electrons) and the Hartree (i.e., classical Coulomb) potential energy can be expressed easily through the electron density:

$$E_{\text{ion}}[n] = \int d^3\mathbf{r} V_{\text{ion}}(\mathbf{r}) n(\mathbf{r}) \quad E_{\text{Hartree}}[n] = \frac{1}{2} \int d^3\mathbf{r}' d^3\mathbf{r} V_{\text{ee}}(\mathbf{r}-\mathbf{r}') n(\mathbf{r}') n(\mathbf{r})$$

□ Using the kinetic energy functional, all of the difficulty of electron-electron interactions is absorbed into the exchange-correlation term:

$$E[n] = E_{\text{kin}}[n] + E_{\text{ion}}[n] + E_{\text{Hartree}}[n] + E_{\text{xc}}[n]$$

Although the exact form of $E_{\text{xc}}[n]$ is unknown, an important aspect of DFT is that the functional $E[n] - E_{\text{ion}}[n]$ does not depend on the material investigated, so that if we knew the DFT functional for one material, we could calculate all materials by simply adding $E_{\text{ion}}[n]$.

□ To calculate the ground-state energy and density, we have to minimize:

$$\frac{\delta}{\delta n(\mathbf{r})} \left\{ E[n] - \lambda \left(\int d^3\mathbf{r} \rho(\mathbf{r}) - N \right) \right\} = 0 \xrightarrow{\text{Kohn-Sham}} \frac{\delta}{\delta \varphi_i(\mathbf{r})} \left\{ E[n] - \varepsilon_i \left[\int d^3\mathbf{r} |\varphi_i(\mathbf{r})|^2 \right] - 1 \right\} = 0$$

$$n(\mathbf{r}) = \sum_{i=1}^N |\varphi_i(\mathbf{r})|^2$$

Kohn-Sham: Electron density expressed in terms of auxiliary one-particle wave function

$$\left[-\frac{\hbar^2}{2m_e} \Delta + V_{\text{ion}}(\mathbf{r}) + \int d^3\mathbf{r}' V_{\text{ee}}(\mathbf{r}-\mathbf{r}') n(\mathbf{r}') + \frac{\delta E_{\text{xc}}[n]}{\delta n(\mathbf{r})} \right] \varphi_i(\mathbf{r}) = \varepsilon_i \varphi_i(\mathbf{r})$$

Kohn-Sham: The final result is a set of one-particle Schrödinger equations describing single electrons moving in time-averaged potential of all electrons

Kohn-Sham Equations in the Local Density Approximation (LDA)

□ The one-particle Kohn-Sham equations, in principle, only serve the purpose of minimizing the DFT energy, **and have no physical meaning**.

□ If we knew the exact $E_{xc}[n]$, which is non-local in $n(\mathbf{r})$, we would obtain the exact ground state energy and density. In practice, one has to make approximations to $E_{xc}[n]$ such as the LDA:

$$E_{xc}[n] \stackrel{\text{LDA}}{\approx} \int d^3\mathbf{r} E_{xc}^{\text{LDA}}(n(\mathbf{r}))$$

$E_{xc}^{\text{LDA}}[n(\mathbf{r})]$ is typically calculated from the perturbative solution or the numerical simulation of the jellium model which is defined by $V_{\text{ion}}(\mathbf{r}) = \text{const}$. Owing to translational symmetry, the jellium model has a constant electron density $n(\mathbf{r}) = n_0$. Hence, with the correct jellium $E_{xc}^{\text{LDA}}[n(\mathbf{r})]$, we could calculate the energy of any material with a constant electron density exactly. However, for real materials $n(\mathbf{r})$ is varying, less so for s and p valence electrons but strongly for d and f electrons.

NOTE: The kinetic energy in KS equations is that of independent (uncorrelated) electrons. The true kinetic energy functional for the many-body problem is different. We hence have to add the difference between the true kinetic energy functional for the many-body problem and the above uncorrelated kinetic energy to E_{xc} so that all many-body difficulties are buried in E_{xc} .

$$E_{\text{kin}}[n_{\text{min}}] = - \sum_{i=1}^N \langle \varphi_i | \hbar^2 \Delta / (2m_e) | \varphi_i \rangle$$

Kohn-Sham "Quasiparticles" and Exchange vs. Exchange-Correlation Hole

Wave function of two non-interacting electrons

$$\Psi_{ij} = \frac{1}{\sqrt{2V}} (e^{i\mathbf{k}_i \cdot \mathbf{r}_i} e^{i\mathbf{k}_j \cdot \mathbf{r}_j} - e^{i\mathbf{k}_i \cdot \mathbf{r}_j} e^{i\mathbf{k}_j \cdot \mathbf{r}_i}) = \frac{1}{\sqrt{2V}} e^{i(\mathbf{k}_i \cdot \mathbf{r}_i + \mathbf{k}_j \cdot \mathbf{r}_j)} (1 - e^{-i(\mathbf{k}_i - \mathbf{k}_j) \cdot (\mathbf{r}_i - \mathbf{r}_j)})$$

$$|\Psi_{ij}|^2 d\mathbf{r}_i d\mathbf{r}_j = \frac{1}{V^2} [1 - \cos(\mathbf{k}_i - \mathbf{k}_j) \cdot (\mathbf{r}_i - \mathbf{r}_j)] d\mathbf{r}_i d\mathbf{r}_j$$

Probability to find electron i in some small volume $d\mathbf{r}_i$ while electron j is in some small volume $d\mathbf{r}_j$

$$P(r)_{\uparrow\uparrow} d\mathbf{r} = n_{\uparrow} [1 - \cos(\mathbf{k}_i - \mathbf{k}_j) \cdot \mathbf{r}]_{\text{aver over FS}} \Leftrightarrow n_{\text{ex}}(\mathbf{r}) = en/2 [1 - \cos(\mathbf{k}_i - \mathbf{k}_j) \cdot \mathbf{r}]_{\text{aver over FS}}$$

$$n_{\text{eff}}(\mathbf{r}) = en/2 + n_{\text{ex}}(\mathbf{r}) = en \left[1 - \frac{9}{2} \frac{(\sin k_F r - k_F r \cos k_F r)^2}{(k_F r)^6} \right]$$

Effective charge density seen by an electron of a given spin orientation in a non-interacting electron gas

PHYSICAL REVIEW B 69, 233105 (2004)

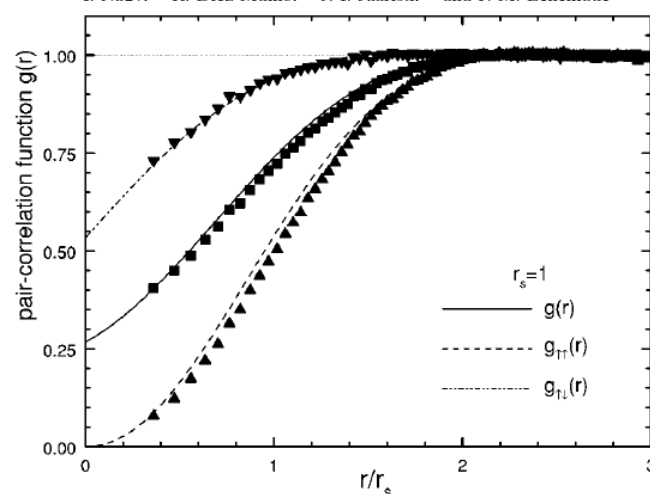
VOLUME 87, NUMBER 3

PHYSICAL REVIEW LETTERS

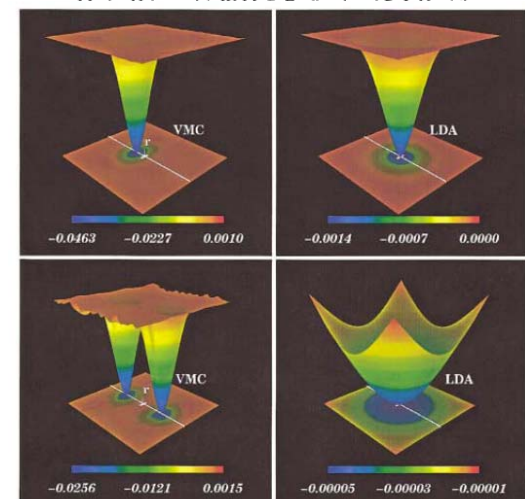
16 JULY 2001

Spin-resolved pair-distribution functions in an electron gas: A scattering approach based on consistent potentials

I. Naev,^{1,2} R. Diez Muño,^{2,3} J. I. Juaristi,^{3,4} and P. M. Echenique^{2,3,4}



Quantum Monte Carlo Analysis of Exchange and Correlation in the Strongly Inhomogeneous Electron Gas



Practical DFT: Pseudopotentials

If we knew the DFT functional for one material, we could treat all materials by simply adding ionic potential which is typically approximated by pseudopotentials.

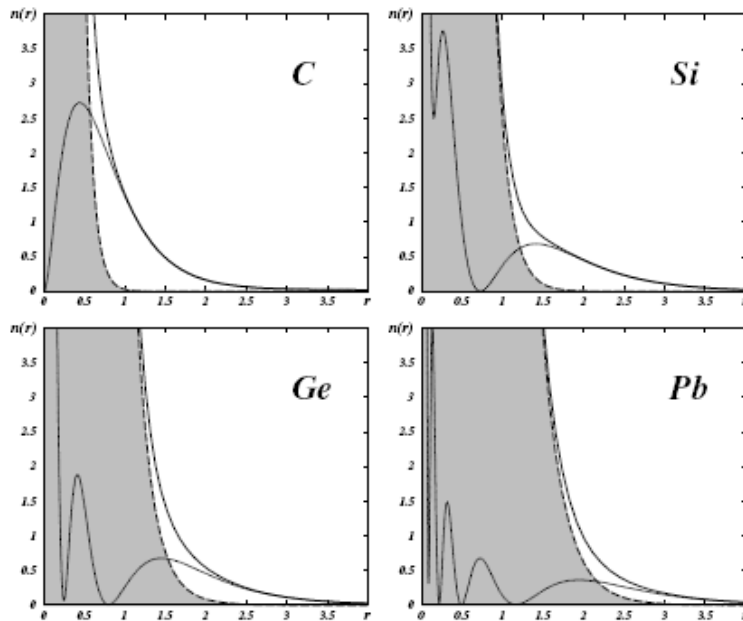
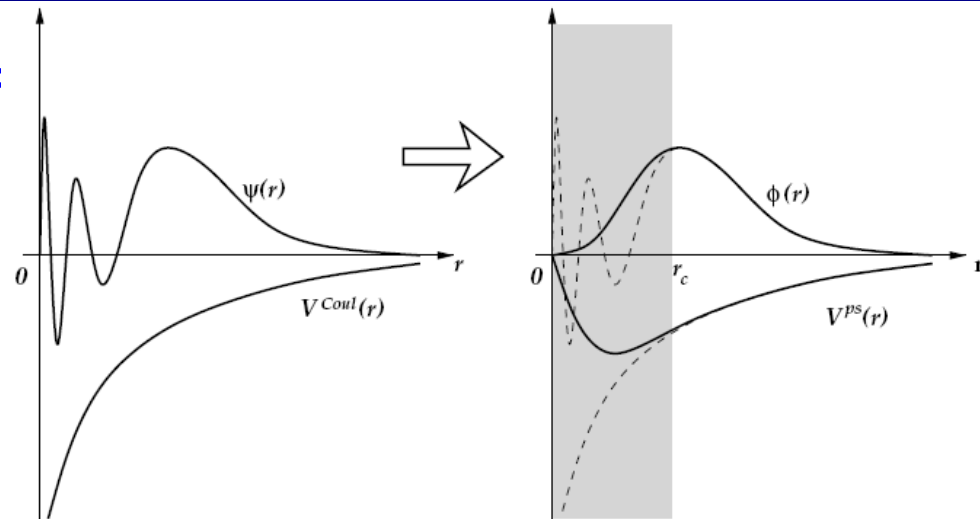


Figure 2.4. Electron densities $n(r)$ as a function of the radial distance from the nucleus r in angstroms, for four elements of column IV of the Periodic Table: C ($Z = 6$, $[1s^2]2s^2 2p^2$), Si ($Z = 14$, $[1s^2 2s^2 2p^6]3s^2 3p^2$), Ge ($Z = 32$, $[1s^2 2s^2 2p^6 3s^2 3p^6 3d^{10}]4s^2 4p^2$) and Pb ($Z = 82$, $[1s^2 2s^2 2p^6 3s^2 3p^6 3d^{10} 4s^2 4p^6 4d^{10} 4f^{14} 5s^2 5p^6 5d^{10}]6s^2 6p^2$); the core states are given inside square brackets. In each case, the dashed line with the shaded area underneath it represents the density of core electrons, while the solid line represents the density of valence electrons and the total density of electrons (core plus valence). The core electron density for C is confined approximately below 1.0 Å, for Si below 1.5 Å, for Ge below 2.0 Å, and for Pb below 2.5 Å. In all cases the valence electron density extends well beyond the range of the core electron density and is relatively small within the core. The wiggles that develop in the valence electron densities for Si, Ge and Pb are due to the nodes of the corresponding wavefunctions, which acquire oscillations in order to become orthogonal to core states.



$$\text{Solve } H^{sp} \psi^{(v)}(r) = [\hat{F} + V^{Coul}(r)] \psi^{(v)}(r) = \epsilon^{(v)} \psi^{(v)}(r)$$

↓

$$\text{Fix pseudo-wavefunction } \phi^{(v)}(r) = \psi^{(v)}(r) \text{ for } r \geq r_c$$

↓

Construct $\phi^{(v)}(r)$ for $0 \leq r < r_c$, under the following conditions:

$$\phi^{(v)}(r) \text{ smooth, nodeless; } d\phi^{(v)}/dr, d^2\phi^{(v)}/dr^2 \text{ continuous at } r_c$$

↓

$$\text{Normalize pseudo-wavefunction } \phi^{(v)}(r) \text{ for } 0 \leq r < \infty$$

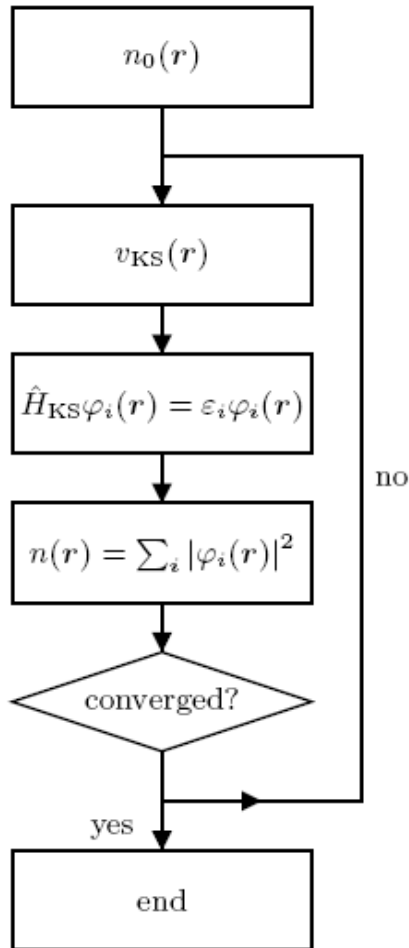
↓

$$\text{Invert } [\hat{F} + V^{ps}(r)] \phi^{(v)}(r) = \epsilon^{(v)} \phi^{(v)}(r)$$

↓

$$V^{ps}(r) = \epsilon^{(v)} - [\hat{F} \phi^{(v)}(r)] / \phi^{(v)}(r)$$

Solving Kohn-Sham Equations via Self-Consistent Loop



A linear-scaling density-functional method

Home

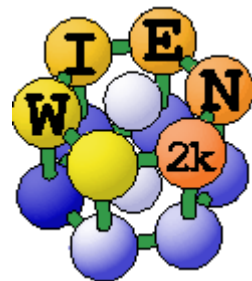
The Siesta Project

Licenses

Documentation

Mailing List

Publications



www.flapw.de
fleur

abinit.org

Interpreting the Hopping Parameters of the Tight-Binding Model of Graphene

□ Transform Hamiltonian matrix elements from coordinate representation into the local orbital basis representation:

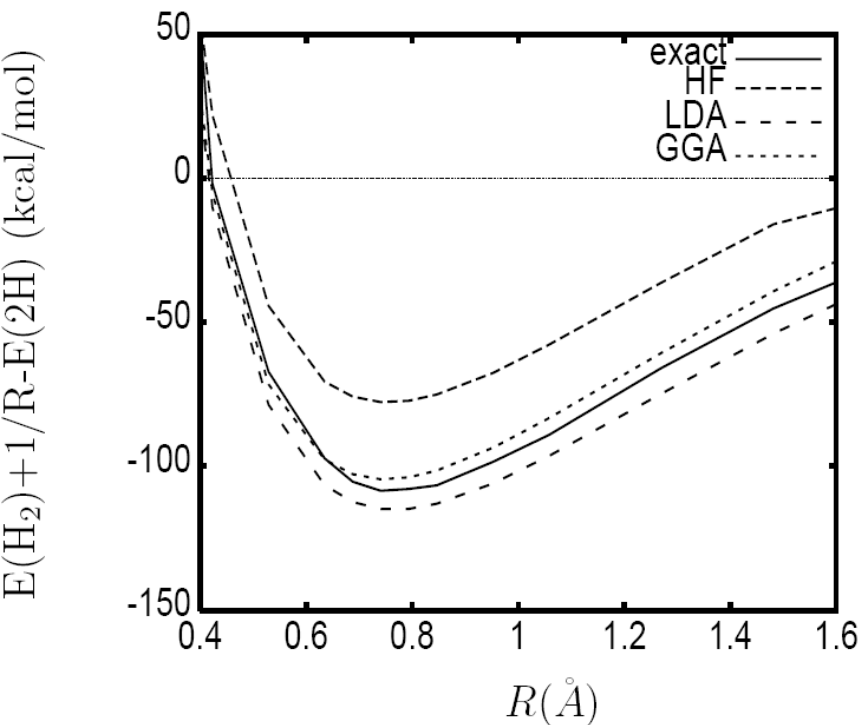
$$t_{il,jm} = \langle il | \hat{H} | jm \rangle \rightarrow t_{il,jm} = \iint d^3\mathbf{r} d^3\mathbf{r}' \langle il | \mathbf{r} \rangle \langle \mathbf{r} | \hat{H} | \mathbf{r}' \rangle \langle \mathbf{r}' | jm \rangle$$

$$t_{il,jm} = \int d^3\mathbf{r} \phi_{il}(\mathbf{r}) \left[-\frac{\hbar^2 \Delta}{2m_e} + V_{\text{ion}}(\mathbf{r}) + \int d^3\mathbf{r}' n(\mathbf{r}') V_{\text{ee}}(\mathbf{r} - \mathbf{r}') + \frac{\partial E_{\text{xc}}^{\text{LDA}}(n(\mathbf{r}))}{\partial n(\mathbf{r})} \right] \phi_{jm}(\mathbf{r})$$

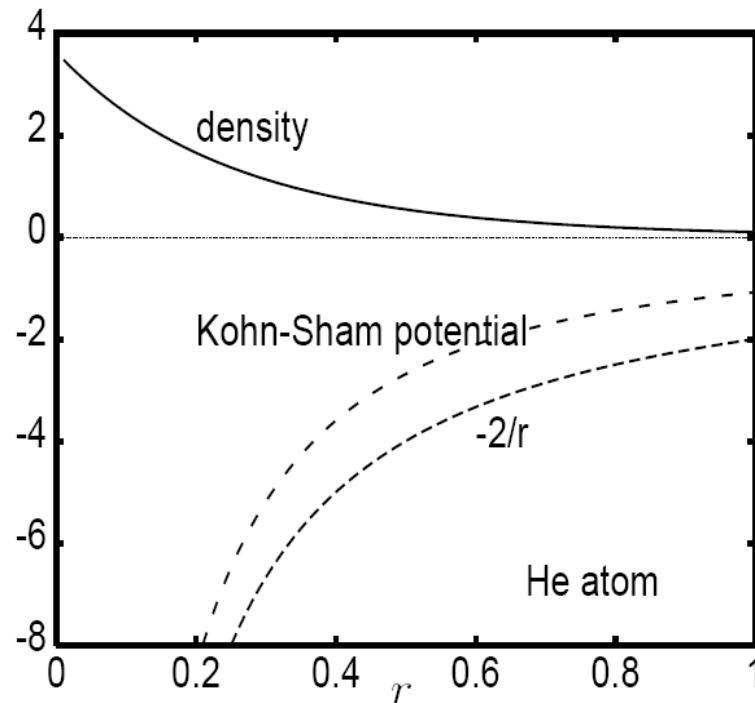
$$\epsilon_{lm}^{\text{LDA}}(\mathbf{k}) = \frac{1}{N} \sum_{ij} t_{il,jm} e^{i\mathbf{k} \cdot (\mathbf{R}_i - \mathbf{R}_j)}$$

l, m denote the orbital index which, for problems with more than one atom in the unit cell, will also index orbitals on different sites in this unit cell

Examples: DFT Applied to 0D Quantum Systems



<http://dft.uci.edu/dftbook.html>



LDA is the simplest possible density functional approximation, and it already greatly improves on Hartree-Fock, although it typically overbinds by about 1 eV (which is too inaccurate for most quantum chemical purposes, but sufficiently reliable for many solid-state calculations). More sophisticated GGA (and hybrids) reduce the typical error in LDA by about a factor of 5 (or more).

Two non-interacting electrons sitting in this potential have precisely the same density as the interacting electrons in **He atom**. If we can figure out some way to approximate this potential accurately, we have a much less demanding set of equations to solve than those of the true system.

Many-Body Perturbation Theory and LDA+GW Approximation

PHYSICAL REVIEW B **78**, 205425 (2008)

Tight-binding description of the quasiparticle dispersion of graphite and few-layer graphene

A. Grüneis,^{1,2,*} C. Attaccalite,^{3,4} L. Wirtz,⁴ H. Shiozawa,⁵ R. Saito,⁶ T. Pichler,¹ and A. Rubio³

¹Faculty of Physics, University of Vienna, Strudlhofgasse 4, 1090 Wien, Austria

²IFW Dresden, P.O. Box 270116, D-01171 Dresden, Germany

³Departamento de Física de Materiales, Donostia International Physics Center, Spain European Theoretical Spectroscopy Facility (ETSF), E-20018 San Sebastian, Spain

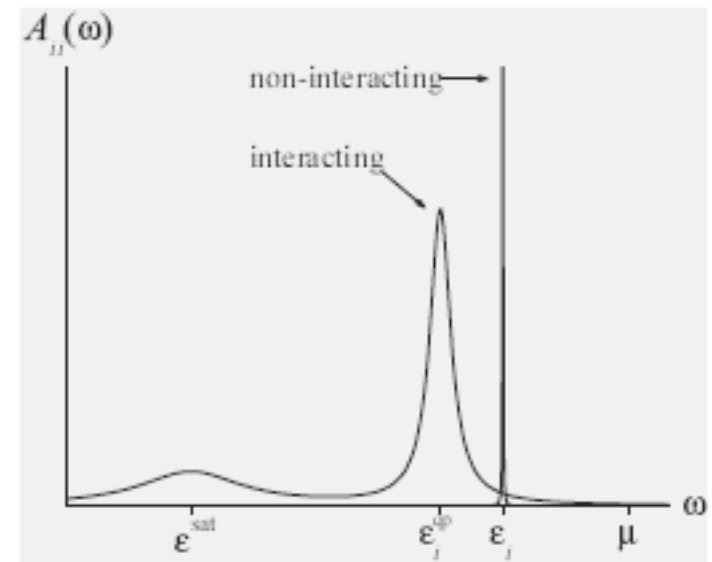
⁴Institute for Electronics, Microelectronics, and Nanotechnology (CNRS UMR 8520), Department ISEN, 59652 Villeneuve d'Ascq, France

⁵Advanced Technology Institute, University of Surrey, Guildford, GU2 7XH, United Kingdom

⁶Department of Physics, Tohoku University, Aoba, Sendai, 980-8578, Japan

(Received 9 August 2008; revised manuscript received 13 October 2008; published 19 November 2008)

A universal set of third-nearest-neighbor tight-binding (TB) parameters is presented for calculation of the quasiparticle (QP) dispersion of N stacked sp^2 graphene layers ($N=1 \dots \infty$) with AB stacking sequence. The present TB parameters are fit to *ab initio* calculations on the GW level and are universal, allowing to describe the whole π “experimental” band structure with one set of parameters. This is important for describing both low-energy electronic transport and high-energy optical properties of graphene layers. The QP bands are strongly renormalized by electron-electron interactions, which results in a 20% increase in the nearest-neighbor in-plane and out-of-plane TB parameters when compared to band structure from density-functional theory. With the new set of TB parameters we determine the Fermi surface and evaluate exciton energies, charge carrier plasmon frequencies, and the conductivities which are relevant for recent angle-resolved photoemission, optical, electron energy loss, and transport measurements. A comparison of these quantities to experiments yields an excellent agreement. Furthermore we discuss the transition from few-layer graphene to graphite and a semimetal to metal transition in a TB framework.



\hat{H}_0 is the (Hermitian) Hamiltonian of a single particle in external potential of ions and classical Hartree potential

$$\hat{H}_0 \phi_i^{qp}(\mathbf{r}) + \int d\mathbf{r}' \hat{\Sigma}(\mathbf{r}, \mathbf{r}'; E_i^{qp}) \phi_n^{qp}(\mathbf{r}') = E_i^{qp} \phi_n^{qp}(\mathbf{r})$$

The total quasiparticle Hamiltonian is non-Hermitian!

$$E_n^{qp} \simeq \varepsilon_n^{KS} + \langle \phi_n | \Sigma(\varepsilon_n^{KS}) - v_{xc} - \Delta\mu | \phi_n \rangle$$

In many cases there is an almost complete overlap between the QP and the KS wavefunctions, and the full resolution of the QP equation may be circumvented by computing the quasiparticle energy using a first-order perturbation of the KS energy.

Coulomb Interaction Effects in Bulk Solids Beyond LDA

Advances in Physics,
Vol. 56, No. 6, November–December 2007, 829–926



Electronic structure calculations using dynamical mean field theory

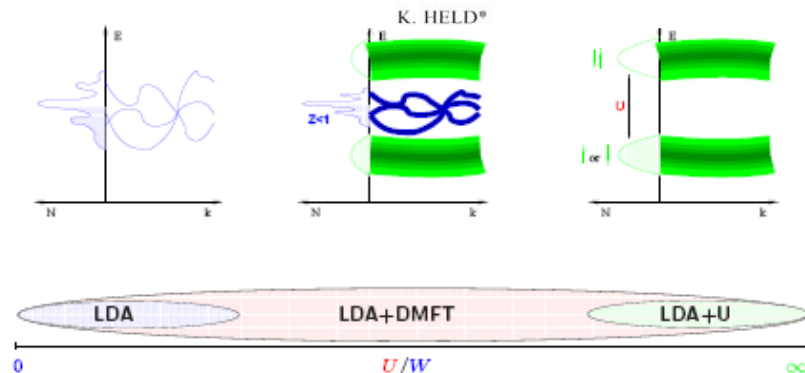


Figure 2.

Weakly correlated metal:
The on-site Coulomb interaction is weak compared to the LDA bandwidth: $U \ll W$; and LDA gives the correct answer, typically a (weakly correlated) metal for which we schematically draw a density of states N at energies E and the bandstructure, i.e. E vs. wave vector k .

Strongly correlated metal:
In this intermediate regime, one has already Hubbard bands, like for $U/W \gg 1$ (right hand side), but at the same time a remainder of the weakly correlated LDA metal (left hand side), in form of a quasiparticle peak: The ($U=0$) LDA bandstructure is reproduced, albeit with its width and weight reduced by a factor Z and life time effects which result in a Lorentzian broadening of the quasiparticle levels.

Mott insulator:
If the Coulomb interaction U becomes large ($U \gg W$), the LDA band splits into two Hubbard bands, and we have a Mott insulator with only the lower band occupied (at integer fillings). Such a splitting can be described by the so-called LDA+ U method with the drawbacks discussed in the text.

The success of LDA shows that this treatment is actually sufficient for many materials, both for calculating ground state energies and band structures, implying that electronic correlations are rather weak in these materials. But, there are important classes of materials where LDA fails, such as transition metal oxides or heavy fermion systems. In these materials the valence orbitals are the 3d and 4f orbitals. For two electrons in these orbitals the distance is particularly short, and electronic correlations particularly strong.

Many such transition metal oxides are Mott insulators, where the on-(lattice-)site Coulomb repulsion U splits the LDA bands into two sets of Hubbard bands. One can envisage the lower Hubbard band as consisting of all states with one electron on every lattice site and the upper Hubbard band as those states where two electrons are on the same lattice site. Since it costs an energy U to have two electrons on the same lattice sites, the latter states are completely empty and the former completely filled with a gap of size U in-between. Other transition metal oxides and heavy fermion systems are strongly correlated metals, with heavy quasiparticles at the Fermi energy, described by an effective mass or inverse weight $m/m_0=1/Z \gg 1$.

Coulomb Interaction Effects in Nanostructures Beyond LDA

Ensslin Lab, APL 92, 012102 (2008)

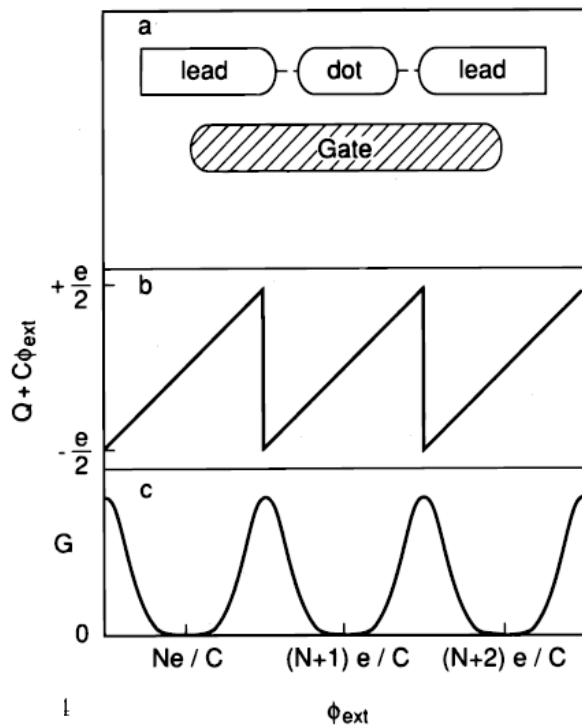
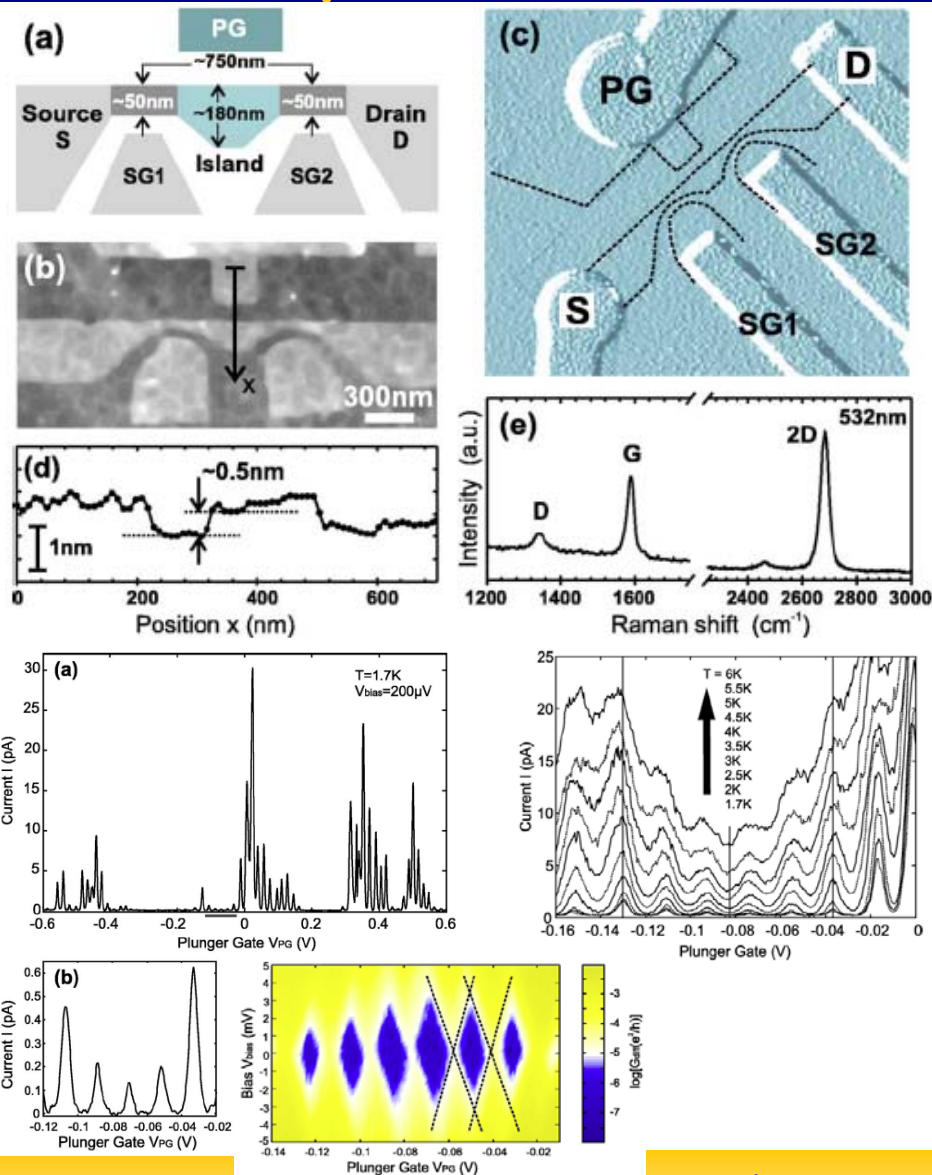


FIG. 1 (a) Schematic illustration of a confined region (dot) which is weakly coupled by tunnel barriers to two leads. (b) Because the charge $Q = -Ne$ on the dot can only change by multiples of the elementary charge e , a charge imbalance $Q + C\phi_{\text{ext}}$ arises between the dot and the leads. This charge imbalance oscillates in a saw-tooth pattern as the electrostatic potential ϕ_{ext} is varied (ϕ_{ext} is proportional to the gate voltage). (c) Tunneling is possible only near the charge-degeneracy points of the saw-tooth, so that the conductance G exhibits oscillations. These are the “Coulomb-blockade oscillations”.



H. van Houten, C. W. J. Beenakker, and A. A. M. Staring, cond-mat/0508454